Thermodynamic analysis of a solar flat plate water heater using extended surface absorber tube

K.Balaji [a], S.Iniyan[a*] and A.Idrish khan [a]
[a] Dept. of Mechanical Engineering, Anna University, Chennai 600 025, India
mr.kbalaj@gmail.com, iniyan777@hotmail.com , idrish92@gmail.com.

Abstract

This paper studies the effect of an absorber tube with and without an extended surface of a solar flat plate water heater. The investigation of this system is carried out using with data acquisition system. Here, a tube and rod are used as an extended surface inside an absorber tube. The extended surfaces are frictionally engaged with the inner side of the tube wall, and it is kept in the axial flow direction of the fluid flow path. The various performance factors such as friction factor and non-dimensional numbers are analyzed. The results show that the outlet temperature of the extended surface absorber tube collector is 8 °C higher when compared to the plain tube collector. Also, it was found that the rod extended surface gives a higher outlet temperature when compared to the tube extended surface. While there was low friction loss, no impact on the pressure drop was found using extended surface inside the absorbing tube.

.

Keywords: Solar flat plate water heater, extended surface absorber tube, non-dimensional number

1. Introduction

Solar flat plate water heating system plays a dynamic role in using solar energy. Active and passive techniques are used for enhancing the heat transfer rate in this system. Nowadays researchers are trying to modify the system and heat transfer fluid (passive), both of which play a vital role in enhancing the efficiency of the collector. The passive technique involves using helical, spiral and curved shaped tubes, twisted tape, micro and longitudinal fins apart from nanofluids. The performances of the systems are analyzed based on the flow type, non-dimensional number, thermal performance, the effect of friction and so on.

[1] This review paper highlights the work done using helical, spiral and curved shaped tubes for both single-phase and two-phase fluids. As much as single-phase heat transfer studies have been reported for the above-mentioned passive types; two-phase heat transfer characteristics have rarely been reported. Most of the work has been done for flow characteristics and pressure drop. [2-7] Different types of twisted tape inside an absorber tube have been worked for achieving better heat transfer rate. Several performance factors like friction factor, pressure drop and heat transfer have been analyzed experimentally and computationally. The effect of natural and forced circulation of heat transfer fluid has been reported using single-phase flow. Here, there are two types of twisted tapes used inside an absorber tube with different configurations namely - trailing edge and helical, which are subjected to comparison. In the helical twisted tape, for various twist angles of **3 to 7**, the heat transfer and the pressure drop were found to be increased.

The Nusselt number correlation was analyzed for the trailing edge twisted tape (comprising of full-length twist, twist with rod and spacer fitted at the trailing edge for lengths of 100, 200 and 300mm for twist angles of **3 – 5**). It was reported that the spacer fitted was better than all other configurations. The author also developed a new correlations for various twisted absorber tubes. The trail edge twisted tape was found to give better results than that of the helical twisted tape. Compared to the plain tube, the overall thermal efficiency enhancement lied from 38.7% to 53.3% at an increased pressure drop of 8.9%. [8, 9] The twisted tape attached with a wire nail and V-cut and their performance factors were evaluated and reported. While the heat transfer in these configurations was higher than the normal twisted tape, both these configurations have not been compared amongst themselves. In the above research works, the performance factors have been analyzed, and it has been reported that there was an enhancement of heat transfer while using twisted tapes. The ratio of pitch to diameter is an important parameter for twisted tapes, and it decreases with increasing pressure drop and heat transfer rate.

doi:10.18086/swc.2015.10.13 Available at http://proceedings.ises.org

[10] The simulation on the circular tube edge fold twisted tape was done, from which the thermal and hydraulic behavior were studied. The increase in the heat transfer in this case was accounted because of the tangential velocity and asymmetrical velocity profile. [11, 12] Thermal performance and friction factor have been analyzed using nanofluids with different twisted tapes and micro fins. Micro finned tube with double twisted tapes gave much higher heat transfer rate than all other types using nanofluids. This paper does not focus on the effect of pressure drop. [13] The experimental investigation on air gap for solar water heater using honeycomb structure with different bottom arrangement has been done. The results indicated that a 3mm gap from the bottom for a single honeycomb unit gave optimum results. Heat removal factor and collector efficiency factors were defined using uncertainty analysis and were compared with experimental data. [14] Theoretical analysis was performed to study the entropy generation and pressure drop for the solar collector with passive technique. The heat transfer fluid was used with metal oxides of nanoparticle at various volume fractions. The exergy destruction has been analyzed based on entropy generation for CuO nanoparticle. The entropy generation is less for CuO than that of other nanoparticle metal oxides. [15] Circular tube with longitudinal fins has been analyzed experimentally. It has been reported, that higher pressure drop occurs in staggered arrangement compared to continuous fin. [16, 17] The efficiency of the collector was theoretically and experimentally reported for sheet and tube solar water heater using rectangular duct and fin. The above analysis states that there is an enhancement of heat transfer when using staggered arrangement on absorber tube for various profiles. The objective of the present work is to design the solar water heater with low heat transfer resistance between the absorbent and absorber tube in order to increase the convective heat transfer coefficient without affecting the flow of an absorbent.

2. Experimental setup and data acquisition

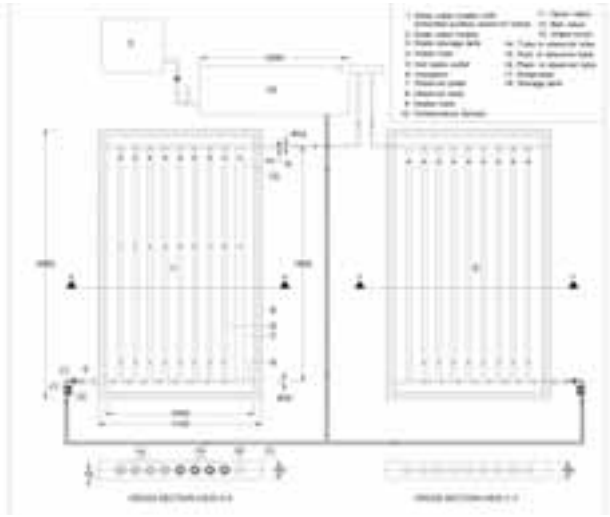

Fig: 1 Top view of solar water heater with and without modification

The study was carried out at the Institute for Energy Studies, Anna University, Chennai. The solar water heater collector was designed for 2 m^2 as per the dimensions are shown in Table.1.

a. Fig.1 shows two water heaters - one with (1) and one without modification (2). Open loop system was used.
b. Both flat plate solar collectors were placed in outdoor condition and oriented towards South with a tilt angle of 13º according to the topographical conditions.
c. The level of the tank was checked every 15 min. The system accelerated the driving force till there was no density difference in the absorbing fluid. The absorber plate absorbed the radiation emitted from the sun, which was transferred through the glass cover.
d. The insulations were provided for minimizing heat loss from the system to the surrounding. The selection of diameter for the extended surface rod and tubes were based on circumference and contact surface.

e. The experiment started at 9.00 am and readings was taken from 10.00 am. Before recording the data, primary work steps were taken like cleaning the glass, removing of residual water from the collectors, and inspecting the collector. The storage tank was filled with clean water every morning at 8.30 am and completely drained in the evening at 5.00 pm.

f. The setup ran from March 28th to May 9th and the following data were recorded at every 5-minute intervals. Measurements were taken multiple times and averaged to reduce experimental error. Solar radiation, ambient temperature, riser tube inlet and outlet temperatures were recorded continuously and averaged for every 30 min interval. On the final day, it was wound that there were a clear peak and deviation in radiation because of which that day was chosen for this study.

g. Thermocouple T – type was used for measuring the temperature with an error of 0.4% to its base value. The thermocouple was placed at each end of the riser tube at a 5mm distance of separation. The intensity of radiation was measured with the help of a pyranometer with an error of ±5% to its base value.

Table.1 Collector parameters

Collector Parameter	**Standards**
Type	Flat plate, 2 m^2, black paint, Single glass, tilt angle 13º.
Heat absorbent fluid	Water
Absorber plate area	1.62 m^2
Sun temperature	4350 K
Optical efficiency of the glass	0.82
Glass thickness	4 mm
Diameter of absorber tube	I.D = 13.8 mm, thickness of 1 mm
Lower and upper header	I.D = 22.3 mm, thickness of 1.5 mm
Insulation width	70 mm
Number of riser tube	9
Connecting pipe	I.D = 25.4 mm
Bottom insulation	Glass wool
Sidewall insulation	Thickness of 5 mm, wood
Absorber plate	Thickness of 4 mm, copper
Tube in tube	O.D = 2.5 mm, t = 0.5 mm, N= 8, L = 1500 mm, Copper
Rod in tube	D = 2.5 mm, N = 8, L = 1500 mm, Copper

3. Data reduction

Thermodynamic and Hydraulic analysis

Assumptions:

- At all the points in the system, the properties of the absorbent remain constant.
- All the processes are in steady state.
- Potential and kinetic energies are neglected.
- There is no soot formation and chemical reaction taking place inside the system.
- There is no mass loss in the absorbent fluid inside the system.

3.1. Energy and Mass balance

$$\sum \dot{E}_{in} = \sum \dot{E}_{out} \quad \text{(eq.1)}$$

$$\sum \dot{m}_{in} = \sum \dot{m}_{out} \quad \text{(eq.2)}$$

Energy balance equation can be expressed as

$$\dot{Q} + \sum \dot{m}_{in}\, \dot{h}_{in} = \dot{W} + \sum \dot{m}_{out}\, \dot{h}_{out} \quad \text{(eq.3)}$$

Whereas, $\dot{Q}_s$ is Available solar energy, expressed by the following equation [7]

$$\dot{Q}_s = I\ A_c \quad \text{(eq.4)}$$

Heat absorbed by the water (absorbing fluid) is

$$Q_{ab} = m\, C_p\, (T_{out} - T_{in}) \quad \text{(eq.5)}$$

3.2. Pressure Drop Analysis

$$\Delta P = f\, \frac{\rho V^2}{2}\, \frac{\Delta l}{d} \quad \text{(eq.6)}$$

$f = \frac{64}{Re}$ For laminar flow

$f = \frac{0.079}{(Re)^{\frac{1}{4}}}$ For turbulent flow

$$V = \frac{\dot{m}}{\rho \frac{\pi}{4} (D_H)^2}$$

Here K is loss coefficient, and D_H is hydraulic diameter

3.3 *Non-Dimensional number*

Nusselt number

$$Nu = \frac{h_i\, D}{K} \quad \text{(eq.7)}$$

$$\frac{1}{U_0 A_0} = \frac{1}{h_i A_i} + \frac{\ln \frac{D_0}{D}}{2\pi\, L\, K_w}$$

Prandtl number

$$Pr = \frac{C_p\, \mu}{K} \quad \text{(eq.8)}$$

Reynolds number

$$Re = \frac{D_i\, \rho\, V}{\mu} \quad \text{(eq.9)}$$

4. Result and discussion

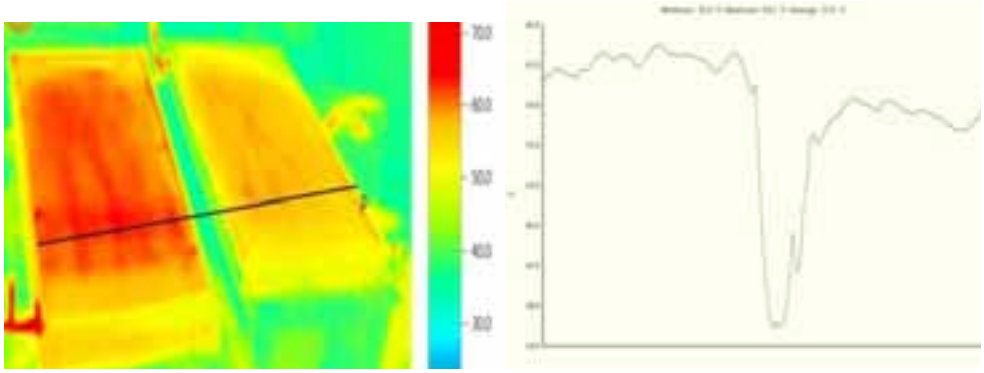

Fig: 2 (a) Thermal image **Fig.2 (b) Profile view**

Fig.2 a and b shows that the temperature of the collector 1 is higher than that of collector 2. In Fig. 2 (b) Profile view, the cross section clearly shows that the peak temperature difference achieved by 8 °C. Testo 875-2 instrument was used for the thermal image. Fig. 2 (a) taken at a reflection temperature of 20 °C. The temperature range was given at the right side of the Fig. 2 (a). The average temperature of the collector 1 and 2 is 62 °C and 54 °C respectively. There is a gap between collector 1 and 2 and it impact on profile view curve. In the profile view, the gap is shown as slag in temperature. The cross section line is drawn at 0.675m from the bottom of the collector. The increase in temperature is due to increase in contact surface area with the axial flow to the water, and the extended surface reduces the thermal and viscous boundary layer. Only at maximum radiation, the maximum temperature difference is achieved. There is no temperature difference between rod and tube extended surface during acceleration and deceleration of radiation. The friction factor is increased for extended surface due to increase in the contact surface with the water. The rod extended surface has higher efficiency than the tube and plain tube configuration in all operating condition because of the thermal mass of the extended surface and friction factor.

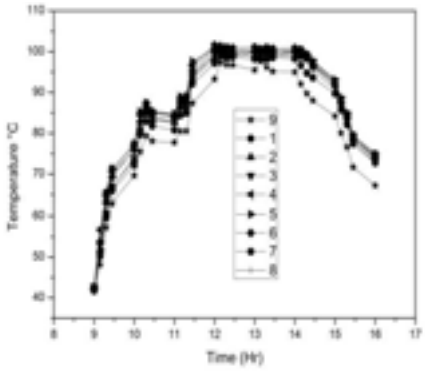

Fig.3: Time Vs Tubes outlet temperature

The arrangement of tubes shown in fig. 1. In Fig.3 first four tubes contain tube extended surface and are compared with a plain tube. Whenever the retardation takes place in radiation, there is a major peak in temperature differences has been achieved. In a constant peak radiation, there are no changes in outlet temperature of the tube. The heat absorbing fluid absorbed the heat, and it changed the phase so the maximum heat capacity achieved by the heat absorbing fluid in a peak radiation. While compared with plain tube there is an average difference in temperature around 8 °C achieved. The result shows that 4th tube gives much better heat transfer compared with other tube because of its focus point. The extended surface increases the wetted surface area which in turn increases the heat extraction from the tube wall to the fluid.

Radiation which fell on earth surface on 9/5/14 is shown in fig 4. There is an unsteady radiation for up to 11.45 am and thereafter gradual retardation took place. Maximum peak achieved at the time of 11.45 am. The collector performance was analyzed for this day because of its unsteady radiation. This graph showed the average temperature of each tube outlet and compared with each other. The tube and rod in extended tube surface show clear performance ranges for different radiations. There was no major deviation in outlet temperature. Whenever the mass flow rate is higher, it affects 1 to 2 °C in each tube. Rod in the tube will result in better performance compared to the tube in tube extended surface. The intensity of solar radiation decreases from 01.00 pm. Hence the heat input to the collector is decreasing. The temperature difference between inlet and outlet decreases gradually which decreases the driving the force. Hence it reduces the instantaneous efficiency of the collector. The instantaneous efficiency is poor in morning and evening may be due to the higher reflection of solar radiation by the glazing which reduces the heat transfer.

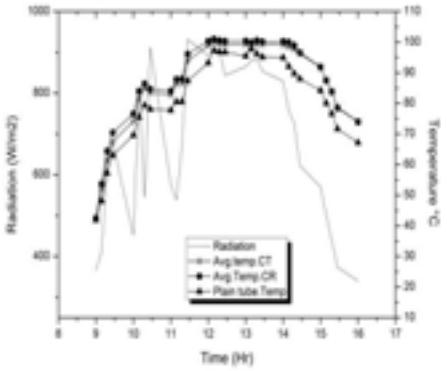

Fig.4 Time Vs Temperature difference with and without extended surface

Fig.5 shows the analysis of the outlet temperatures of both the collector. Collector 1 gives maximum output temperature in a peak radiation. During acceleration and retardation, there are no temperature changes in outlet because of the velocity of the heat absorbing fluid. In a thermosyphon process, the heat absorbing fluid leaves the system only when density difference is high. The velocity of the absorbing fluid is the determining factor for the outlet temperature of the collector. The temperature difference between inlet and outlet temperature is high. The extended surface increases the contact surface area which in turn increases the heat removal from the tube wall to the fluid. Hence there is a gradual increase in the Reynolds number for extended surface which in turn increases the instantaneous efficiency of the collector.

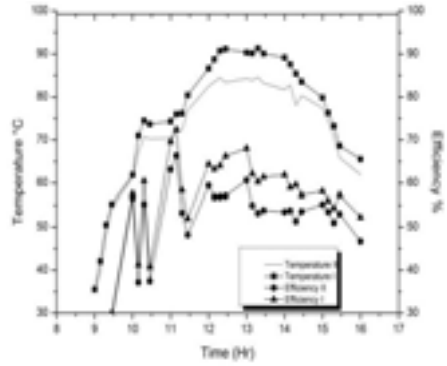

Fig.5: Time Vs Efficiency, Outlet temperature

Fig.6 explain that extended surface at leading edges will enhance the inertia forces of the heat absorbing fluid, so it reduces the viscous boundary layer. The extended surface absorber tube of the rod has maximum velocity than the tube in tube extended surface and plain tube. A thin boundary layer forms nearer to the wall surfaces, and it is stationary with respect to the surface. The thickness of the layer will be reduced when enhancing the velocity of the absorbing fluid till the free stream velocity is reached. There is no boundary layer at free stream velocity.

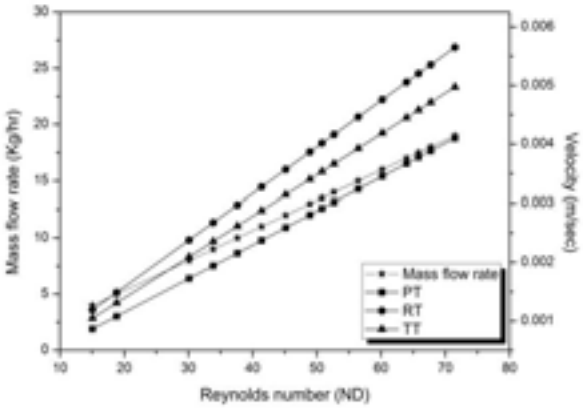

Fig.6: Effect of Reynolds number at different mass flow rate.

Fig.7 gives a clear picture about the relationship between Nusselts number and Reynolds number. When mass flow rate increases, inertia force also increased and reduced the thickness of the viscous boundary layer. It enhances the heat transfer coefficient. The Nusselts number rises with increasing Reynolds number if the mass flow rate is increased. The extended surfaces are frictionally contact with the inner side of the tube wall, and it extends the contact surface of the water flowing through it, so it reduces the plate temperature. The heat removal rate from the absorber plate of the extended surface collector is higher than that of the plain tube collector, and it has the minimum plate temperature. The rate of heat transfer from the absorber tube to water is high for the extended surfaces. The rod extended surface collector has very less absorber plate temperature than the plain tube and tube extended surface collector at same intensity of radiation due to the mass of the rod extended surface. A stably stratified layer of light and warm water is sustained near the top of the extended surface which absorbs the heat. The warmer water near the bottom of the absorber tube induces the convective motion, and it increases the velocity. A thin boundary layer forms near the wall, and it is stationary with respect to the surface. Buoyance force removes the energy from the fluid, higher than shear force. The turbulence is damped against the buoyancy force, and the heat transfer is entirely due to laminar flow in flat plate collector. Free convection increases with increase in the Nusselt number, and it is dominating the performance of the collector. Free convection is stronger when the Reynolds number is low. Due to increase in contact surface, the extended surface has higher Nusselt number.

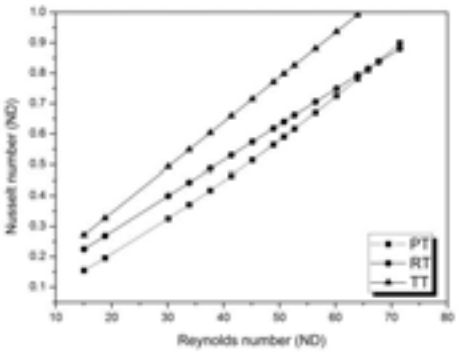

Fig. 7: Effect of Reynolds number on heat transfer

Fig. 8 shows the variation of friction factor with respective to the Reynolds number. Darcy friction factor is derived with the help of velocity of the flowing fluid inside the tube. Darcy friction only for tubes inside the collector. The viscous boundary layer is hampering the absorbing fluid velocity, and it will reduce Reynolds number. The pressure drop is measured for entire collector using head losses, and it is used for measuring the fanning friction factor. The extended surfaces have very less enhancement in friction factor compared to other types of heat transfer enhancement devices like twisted tape and grooved tube. Because of this extended surfaces are frictionally engaged with the inner wall, and it is fixed with the axial flow direction of the water. These heat transfer enhancement devices are highly suitable for the passive technique. As it is evident from the figure, the higher pressure drop is obtained for higher Reynolds number, and it decreases with a decrease in the flow rate.

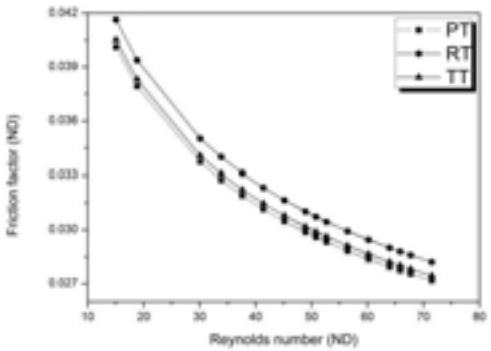

Fig.8: Effect of Reynolds number on viscous of the absorbing fluid

Fig.9 clearly shows the deviation of theoretical outlet temperature with experimental. Maximum deviation between the experimental and theoretical data was 10%. The theoretical outlet temperature of the collector does not consider the thermal loss inside the collector, so the value is higher than experimental.

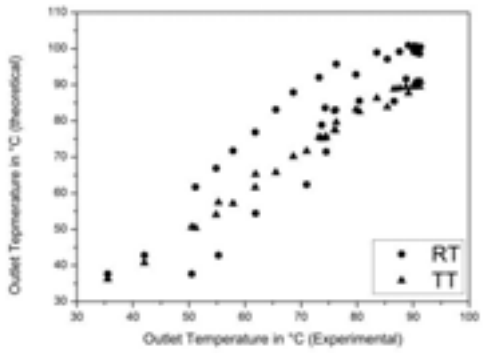

Fig.9: Comparison of experimental and theoretical outlet temperature data of the collector

5. Conclusion.

The experimental study of solar water heater with extended surface absorber tube was performed, and the Rod extended surface provides higher heat transfer rate compared to Tube extended surface because of the mass flux of the extended surface. Extended surface reduces the thermal and viscous boundary layer, so it increases the convective heat transfer rate. The velocity is increased by means of increasing the shear production, and the extended surfaces have been found to be effective in augmenting the heat transfer. The efficiency of the modified collector is increased by 22%. Extended surface also increases the non-dimensional numbers and friction factor.

Nomenclature

A_c	Collector area, m^2
C_p	Specific heat, $Jkg^{-1}K^{-1}$
D_h	Hydraulic diameter, m
f	Friction factor, Non dimension
I	Intensity of radiation, Wm^{-2}
k	Thermal conductivity, $W\ m^{-1}K^{-1}$
k_i	Thermal conductivity of insulation material $W\ m^{-1}K^{-1}$
k_w	Thermal conductivity of the tube wall, $W\ m^{-1}K^{-1}$
L	Length of the tube, m
m	mass flow rate, kgs^{-1}
N	Number of tubes, Nondimension
Nu	Nusselt number, Nondimension
Pr	Prandtl number, Nondimension
Re	Reynolds number, Nondimension
Q_{ab}	Heat absorbed, W
T_{Out}	Outlet temperature of the collector, K
T_{in}	Inlet temperature of the collector, K
T_a	Atmospheric temperature, K
V	Velocity, ms^{-1}

Greek Symbol

ρ	Density, kgm^{-3}
μ	Dynamic viscosity, Nsm^{-2}
μ_w	Dynamic viscosity of tube wall, Nsm^{-2}
η	Efficiency, %

Suffix

PT	Plain tube
RT	Rod as extended surface
TT	Tube as extended surface

Reference

[1] Naphon P, Wongwises S. A review of flow and heat transfer characteristics in curved tubes. Renewable and Sustainable Energy Reviews. 2006;10:463-90.
[2] Jaisankar S, Radhakrishnan TK, Sheeba KN. Experimental studies on heat transfer and friction factor characteristics of thermosyphon solar water heater system fitted with spacer at the trailing edge of twisted tapes. Applied Thermal Engineering. 2009;29:1224-31.
[3] Jaisankar S, Radhakrishnan TK, Sheeba KN. Studies on heat transfer and friction factor characteristics of thermosyphon solar water heating system with helical twisted tapes. Energy. 2009;34:1054-64.
[4] Jaisankar S, Radhakrishnan TK, Sheeba KN. Experimental studies on heat transfer and friction factor characteristics of forced circulation solar water heater system fitted with helical twisted tapes. Solar Energy. 2009;83:1943-52.
[5] Jaisankar S, Radhakrishnan TK, Sheeba KN. Experimental studies on heat transfer and thermal performance characteristics of thermosyphon solar water heating system with helical and Left–Right twisted tapes. Energy Conversion and Management. 2011;52:2048-55.
[6] Jaisankar S, Radhakrishnan TK, Sheeba KN, Suresh S. Experimental investigation of heat transfer and friction factor characteristics of thermosyphon solar water heater system fitted with spacer at the trailing edge of Left–Right twisted tapes. Energy Conversion and Management. 2009;50:2638-49.
[7] Ananth J, Jaisankar S. Investigation on heat transfer and friction factor characteristics of thermosiphon solar water heating system with left-right twist regularly spaced with rod and spacer. Energy. 2014;65:357-63.
[8] Murugesan P, Mayilsamy K, Suresh S. Heat Transfer and Friction Factor Studies in a Circular Tube Fitted with Twisted Tape Consisting of Wire-nails. Chinese Journal of Chemical Engineering. 2010;18:1038-42.
[9] Murugesan P, Mayilsamy K, Suresh S, Srinivasan PSS. Heat transfer and pressure drop characteristics in a circular tube fitted with and without V-cut twisted tape insert. International Communications in Heat and Mass Transfer. 2011;38:329-34.
[10] Cui Y-z, Tian M-c. Three-dimensional numerical simulation of thermal-hydraulic performance of a circular tube with edgefold-twisted-tape inserts. Journal of Hydrodynamics, Ser B. 2010;22:662-70.
[11] Eiamsa-ard S, Wongcharee K. Single-phase heat transfer of CuO/water nanofluids in micro-fin tube equipped with dual twisted-tapes. International Communications in Heat and Mass Transfer. 2012;39:1453-9.
[12] Eiamsa-Ard S, Wongcharee K. Heat transfer characteristics in micro-fin tube equipped with double twisted tapes: Effect of twisted tape and micro-fin tube arrangements. Journal of Hydrodynamics, Ser B. 2013;25:205-14.
[13] Abdullah AH, Abou-Ziyan HZ, Ghoneim AA. Thermal performance of flat plate solar collector using various arrangements of compound honeycomb. Energy Conversion and Management. 2003;44:3093-112.
[14] Alim MA, Abdin Z, Saidur R, Hepbasli A, Khairul MA, Rahim NA. Analyses of entropy generation and pressure drop for a conventional flat plate solar collector using different types of metal oxide nanofluids. Energy and Buildings. 2013;66:289-96.
[15] El-Sayed SA, El-Sayed SA, Abdel-Hamid ME, Sadoun MM. Experimental study of turbulent flow inside a circular tube with longitudinal interrupted fins in the streamwise direction. Experimental Thermal and Fluid Science. 1997;15:1-15.
[16] Ho C-D, Chen T-C, Tsai C-J. Experimental and theoretical studies of recyclic flat-plate solar water heaters equipped with rectangle conduits. Renewable Energy. 2010;35:2279-87.
[17] Ho CD, Chen TC. Collector efficiency improvement of recyclic double-pass sheet-and-tube solar water heaters with internal fins attached. Renewable Energy. 2008;33:655-64.